JOURNAL OF APPLIED ELECTROCHEMISTRY 22 (1992) 383–389

The inhibition of corrosion and hydrogen embrittlement of AISI 410 stainless steel

R. AGRAWAL, T. K. G. NAMBOODHIRI

Department of Metallurgical Engineering, Institute of Technology, Banaras Hindu University, Varanasi-221005, India

Received 17 April 1991

A study was carried out on the inhibition of corrosion and hydrogen embrittlement of AISI 410 stainless steel by two organic inhibitors, namely benzotriazole and benzonitrile. Tensile testing, scanning electron microscopy, weight loss measurements and potentiodynamic polarization were the techniques used for this study. Tensile tests showed that 410 steel is highly susceptible to hydrogen stress cracking. Scanning electron microscopic observations of fracture surfaces showed a brittle quasi-cleavage type of failure when the steel was hydrogen charged from 0.5 M H_2SO_4. Both inhibitors reduced hydrogen induced ductility loss though the fracture mode was unaltered. They showed increasing inhibition efficiencies for corrosion as well as cathodic hydrogen evolution as their concentration in H_2SO_4 increased from 3.9×10^{-5} M to 8.4×10^{-3} M. Benzonitrile was found to be a more efficient inhibitor than benzotriazole for AISI 410 stainless steel exposed to 0.5 M H_2SO_4.

1. Introduction

AISI 410 stainless steel is one of the most popular steels amongst the 400 series martensitic stainless steels used in corrosion resistant and high strength applications [1, 2]. 12% Cr martensitic stainless steels like the 410 steel have found wide usage in gas and oil production applications because of their high corrosion resistance in CO_2 containing environments [3, 4]. However, they are susceptible to environmental cracking and localized corrosion in the presence of H_2S [5, 6]. Hydrogen damage has been reported [7] in such steels in the presence of H_2S and acidic conditions, typically observed in gas well and oil production applications.

Hydrogen embrittlement in these steels has been well established by several workers in the past few decades [8–12]. In a recent study [13], hydrogen embrittlement susceptibility of quenched and tempered 12% Cr stainless steel in sulphate, sulphide, chloride and hydroxide solutions was correlated to applied polarization potential [13]. Quenching and tempering in the presence of CO_2 rendered the chromium stainless steel passive and reduced the effects of aggressive environments [14, 15]. Recent studies show that the hydrogen diffusion coefficient increases at tempering temperatures [16]. Air-cooling of this steel from the austenitizing range is the commercial practice [10]. Slow cooling rates through the martensitic range or isothermal holding for even a short time improves the cracking resistance of 410 steel. The annealed martensitic stainless steel has lower internal stress which reduces the failure probability [17].

Inhibitors play an important role in controlling the corrosion of steels and the kinetics of the hydrogen evolution reaction [18–22]. Nitrogen and sulphur containing organic compounds have been traditionally used as corrosion inhibitors [23]. Amongst nitrogen containing compounds benzotriazole (BTA) and benzonitrile have been widely studied as inhibitors in acidic media for high carbon steels, mild steel and HSLA steels [24–27]. In order to minimize the absorption of hydrogen, which arises during acid cleaning of steel components, it is customary to add to the pickle liquor certain organic compounds which serve as inhibitors [28, 29].

In the present investigation the corrosion and hydrogen embrittlement behaviour of 410 stainless steel in 0.5 M H_2SO_4 and its inhibition by various concentrations of BTA and benzonitrile has been studied using tensile testing, scanning electron microscopy, weight loss measurements and cathodic polarization.

2. Experimental procedure

Commercial 2 cm dia. rod stock of AISI 410 stainless steel, with the nominal composition given in Table 1, was used. Standard round tensile specimens, gauge length 15.5 mm and gauge dia 4.4 mm were machined from the as-received material. Cylindrical specimens, 9 mm dia. × 12 mm long, were prepared for polarization studies. Square specimens, 1 cm × 1 cm, were cut from 1 mm thick sheet for weight loss studies. They were austenitized at 980° C for 45 mins and air-cooled to obtain a martensitic structure. All the specimens were polished with emery paper up to 4/0 grade and cleaned with distilled water and acetone.

After weighing the square samples they were suspended in 0.5 M H_2SO_4 containing different concentrations of inhibitors for different intervals of time and their weight losses were determined.

An EG&G PARC model no. 331–3, corrosion

0021-891X/92

Table 1. Nominal composition of AISI 410 stainless steel [2]

Element	*Cr*	*C*	*Mn*	*Si*	*P*	*S*	*Fe*
Wt(%)	11.5–13.5	0.15 max	1.0 max.	1.0 max.	0.040 max.	0.030 max.	Balance

measurements system was used for polarization measurements. The polarization cell contained a graphite counter electrode and a saturated calomel reference electrode. The cathodic polarization curves of the steel were determined in the deaerated electrolyte. Dearation of the electrolyte was carried out for 2 h prior to the start of polarization. All measurements were done at a scanning rate of 1 mV s^{-1}. The sulphuric acid and the inhibitors used were of AnalaR grade and all the solutions were prepared using triple distilled water. All the experiments were performed at room temperature, 34 ± 2° C.

To evaluate the hydrogen embrittlement characteristics, the steel was hydrogen charged cathodically from a solution of 0.5 M H_2SO_4 at a constant current density of 10 mA cm^{-2} using platinum as anode and a constant d.c. power supply. All specimens were charged for 4 h. Slow strain rate tensile testing at a strain rate of 5×10^{-5} s^{-1} were conducted on these specimens in air immediately after charging using a universal testing machine. The effect of inhibitors was tested by hydrogen charging the steel from 0.5 M H_2SO_4 solution containing various concentration of benzotriazole and benzonitrile and doing the tensile test as above. Although the hydrogen charging time of 4 h used in this study was insufficient to fill the tensile specimen completely with hydrogen, it was nevertheless sufficient to cause a change in the stress–strain behaviour of this steel, the magnitude of which was used as an index of the efficiency of the inhibitors. The fractured specimens were observed using a Philips SEM 500 scanning electron microscope to determine the fracture mode.

Table 2. Weight loss data of AISI 410 steel in the presence of inhibitors in 0.5.M H_2SO_4

S. No.	*Inhibitor concentration /mM*	*Time /h*	*Corrosion rate /m.p.y.*	*Efficiency /%*
1.	Without inhibitor	2	1323	
		4	2013	
		6	2044	
		24	2713	
2.	Benzotriazole			
	(a) 0.42	2	373	71.8
		6	541	73.6
		24	675	75.1
	(b) 0.84	2	354	73.2
		6	506	75.2
		24	602	77.8
	(c) 4.2	2	354	73.2
		6	367	82.0
		24	481	82.3
	(d) 8.4	2	205	84.5
		6	267	86.9
		24	352	87.0
3.	Benzonitrile			
	(a) 0.39	2	494	62.7
		4	429	78.7
		6	348	83.0
		24	280	89.7
	(b) 0.974	2	466	64.8
		4	410	79.6
		6	332	83.7
		24	231	91.5
	(c) 4.87	2	419	68.3
		4	373	81.5
		6	286	86.0
		24	190	93.0
	(d) 9.74	2	335	75.0
		4	321	84.0
		6	236	88.4
		24	149	94.5

3. Results

3.1. *Inhibition of corrosion and hydrogen evolution reaction*

3.1.1. Weight loss measurements. Table 2 gives the data obtained from weight loss measurements. It was observed that the corrosion rate increases with time in the uninhibited acid as well as in the acid containing benzotriazole. However, the presence of benzonitrile leads to decreasing corrosion rate with increasing time. In both cases, the corrosion rate decreases with increase in inhibitor concentration. The inhibition

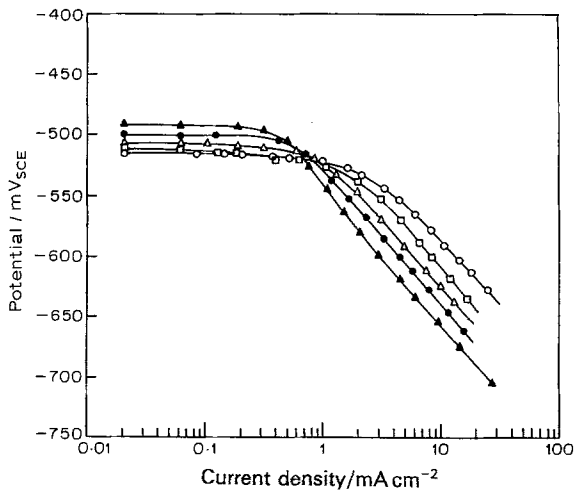

Fig. 1. Variation of the potentiodynamic cathodic polarization curve of AISI 410 steel in 0.5 M H_2SO_4 in the presence of benzotriazole. Temp. 36 ± 3° C; scan rate 1 mV s^{-1}. Benzotriazole concentration: (○) 0.0, (□) 0.17, (△) 0.84, (●) 4.2 and (▲) 8.4 mM.

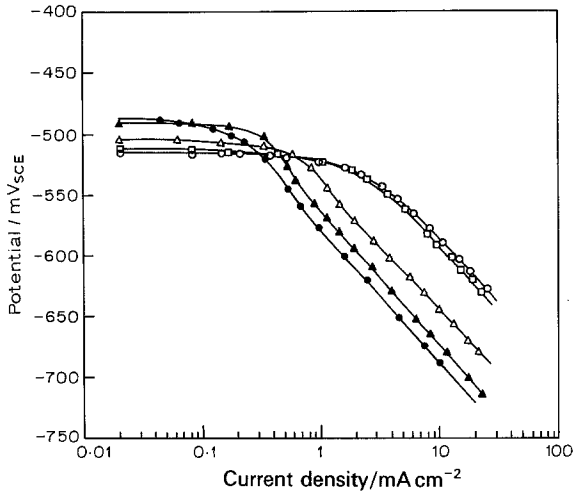

Fig. 2. Variation of the potentiodynamic cathodic polarization curve of AISI 410 steel in 0.5 M H_2SO_4 in the presence of benzonitrile. Temp. 36 ± 3° C; scan rate 1 mV s^{-1}. Benzonitrile concentration: (○) 0.0, (□) 0.039, (△) 0.39, (▲) 0.974 and (●) 4.87 mM.

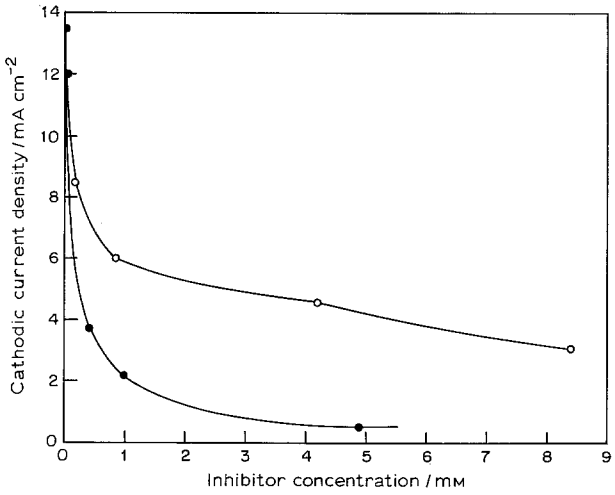

Fig. 3. Effect of benzotriazole and benzonitrile concentration on the cathodic current density at −600 mV of AISI 410 steel in 0.5 M H_2SO_4. Temp. 36 ± 3° C; scan rate 1 mV s^{-1}. At 600 mV: (○) benzotriazole and (●) benzonitrile.

efficiency increases with increase in inhibitor concentration and exposure time for both inhibitors.

3.1.2. Polarization studies. Figures 1 and 2 show the effect of concentrations of benzotriazole and benzonitrile respectively on the cathodic polarization of 410 steel in 0.5 M H_2SO_4. The polarization curves are shifted towards lower current densities and the corrosion potential towards more noble values with increasing inhibitor concentration. The corrosion potentials and the corrosion current densities vary somewhat more in the presence of benzonitrile as compared to those in the presence of BTA as indicated in Table 3.

Table 3 indicates that the corrosion current density and corrosion rate decrease with increasing inhibitor concentration for both BTA and benzonitrile. On the basis of the corrosion current density the inhibition efficiency was calculated using the relation

$$\eta(\%) = \frac{i_u - i_i}{i_u} \times 100 \qquad (1)$$

where, i_u is the corrosion current density in uninhibited corrodent and i_i is the corrosion current density in inhibited corrodent.

Table 3 also shows an increase in inhibition efficiency with increasing concentration of inhibitor. A pronounced concentration effect is seen in corrosion inhibition efficiency, particularly below 1 mM concentration in the case of benzonitrile. The Tafel slopes calculated from Figs 1 and 2 and tabulated in Table 3 show a change from 100 mV per decade for the uninhibited to 110 mV per decade in the case of inhibited acid solutions. This is in agreement with the value reported by Nobe [30]. The average value of the Tafel slope in the presence of BTA is 108 ± 2 mV per decade while in the case of benzonitrile, it is 106 ± 4 mV per decade.

The effect of these inhibitors on the hydrogen evolution reaction on 410 steel exposed to 0.5 M H_2SO_4 was evaluated on the basis of the cathodic current density at the Tafel region. Figure 3 depicts the variation of cathodic current density with inhibitor concentration. Cathodic inhibition efficiency was calculated on the

Table 3. Corrosion parameters obtained from potentiodynamic cathodic polarization curves

S. No.	*Inhibitor concentration /mM*	*Corrosion potential /mV (SCE)*	*Cathodic Tafel slope /mV dec^{-1}*	*Corrosion current density /mA cm^{-2}*	*Corrosion rate /m.p.y.*	*Corrosion inhibition efficiency /%*	*Cathodic (−600 mV) inhibition efficiency /%*
1.	Uninhibited	−515	100.0	1.90	848	-	-
2.	Benzotriazole						
	0.17	−513	107.5	1.30	581	31.6	37.0
	0.84	−507	107.5	0.80	357	57.9	55.6
	4.20	−499	110.0	0.56	250	70.5	66.0
	8.40	−492	108.0	0.32	143	83.2	77.0
3.	Benzonitrile						
	0.039	−512	102.5	1.70	759	10.5	11.1
	0.390	−504	103.5	0.45	201	76.3	72.2
	0.974	−490	110.0	0.22	98	88.4	83.7
	4.870	−487	110.0	0.15	67	92.1	95.7

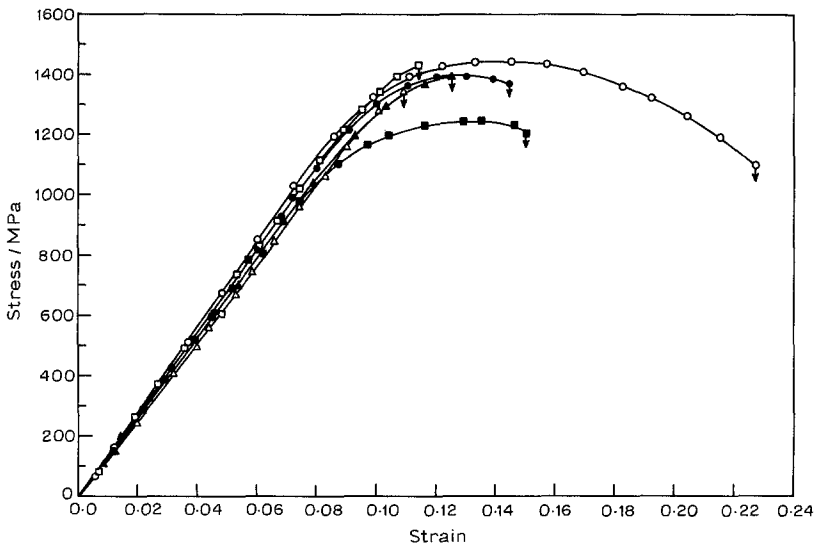

Fig. 4. Tensile stress–strain curves of air-hardened AISI 410 steel after hydrogen charging from 0.5 M H_2SO_4 containing different concentrations of benzotriazole at a current density of 10 mA cm^{-2} for 4 hr. Temp. 34 ± 2° C; strain rate 5 × 10^{-5} s^{-1}. (○) Unchanged. Concentrations m M (△) 0.0, (□) 0.39, (▲) 0.974, (●) 4.87 and (■) 9.74.

basis of cathodic current density. Table 3 clearly indicates that the cathodic inhibition efficiency for h.e.r. increases with increase of inhibitor concentration and the effect is much more pronounced in the case of benzonitrile than for BTA.

3.2. *Inhibition of hydrogen embrittlement*

Figures 4 and 5 show the tensile stress–strain curves for the 410 steel hydrogen charged for 4 h from 0.5 M H_2SO_4 with or without different concentrations of the two inhibitors. It is seen that specimens hydrogen charged from the uninhibited acid failed in a brittle fashion with a total strain of 0.10, which is less than half of the strain at fracture seen in an uncharged specimen. The slope of the stress–strain curve is unaltered by hydrogen charging. This is typical of hydrogen embrittlement in high strength steels [31].

With the addition of inhibitors to the charging medium the ductility of charged specimens is seen to increase in Figs 4 and 5. The initial slopes of these curves are nearly equal for all inhibitor concentrations but the fracture ductility increases at higher inhibitor contents. The relevant tensile parameters obtained from these curves are listed in Table 4. It is seen from the table that hydrogen charging of the hardened 410 steel in 0.5 M H_2SO_4 caused a decrease in UTS and ductility values. When BTA and benzonitrile were used as inhibitors in 0.5 M H_2SO_4, UTS showed a minor decrease but the ductility parameters increased with increasing concentration of inhibitor. The percentage reduction in area increased 15 to 20 times while the percentage elongation increased 2 to 3 times. Even at the highest inhibitor concentration studied here, the ductility values recovered only by 50% of the values for uncharged samples.

The inhibition efficiency for hydrogen embrittlement of the two organic compounds was calculated from tensile ductility values using the relationship,

$$\text{Efficiency, } E(\%) = \frac{\Delta EL' - \Delta El''}{\Delta El'} \times 100 \quad (2)$$

where $\Delta El' = (\%El)_{\text{uncharged}} - (\%El)$ charged from uninhibited acid = change in tensile ductility without inhibitor, and $\Delta El'' = (\%El)_{\text{uncharged}} - (\%El)$ charged from inhibited acid = change in tensile ductility with inhibitor.

As seen from Table 4 the loss in ductility due to

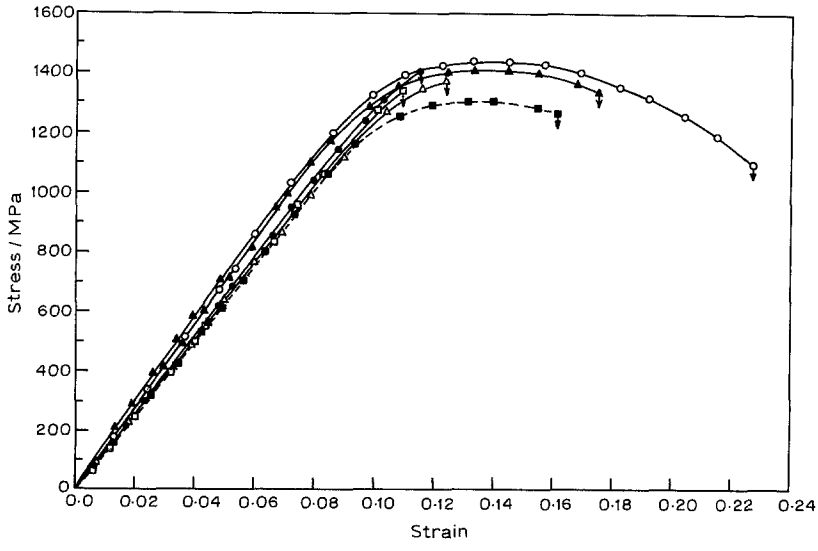

Fig. 5. Tensile stress–strain curves of air-hardened AISI 410 steel after hydrogen charging from 0.5 M H_2SO_4 containing different concentrations of benzonitrile at a current density of 10 mA cm^{-2} for 4 hr. Temp. 34 ± 2° C; strain rate 5 × 10^{-5} s^{-1}. (○) Unchanged. Concentrations m M (□) 0.0, (●) 0.17, (△) 0.84, (■) 4.2 and (▲) 8.4.

hydrogen charging is decreased with increase in inhibitor concentration. The inhibition efficiency for hydrogen embrittlement increased with increasing concentration for both inhibitors. In other words, both inhibitors reduced the hydrogen embrittlement susceptibility of AISI 410 steel.

3.2.1. Fractography. Figure 6 shows fractographs of the uncharged 410 stainless steel. A ductile cup and cone fracture is seen in this figure. The low magnification picture shown in Fig. 6a gives the cup portion of the specimen. It shows a flat central region with radial lines emanating from the centre of the specimen and a peripheral shear lip. The higher magnification picture in Fig. 6b gives details of the ductile fracture due to microvoid coalescence. A distribution of large dimples in a matrix of small dimples is visible in this picture. The large dimples probably originated at inclusions present in this material.

Figure 7 shows the fractographs obtained from 410 steel hydrogen charged from 0.5 M H_2SO_4 for 4 h at a current density of 10 mA cm^{-2}. Hydrogen charging is seen to reduce the ductility of the material drastically as evidenced by the lower reduction in area seen in Fig. 7a in comparison to that shown in Fig. 6a. Here the entire fracture surface is taken up by the flat fracture region indicating the brittleness of the material. Figure 7b gives details of the brittle fracture. The fracture surface contains flat and smooth facets indicative of quasi-cleavage.

The brittle behaviour of the hydrogen charged steel is somewhat reduced by the addition of BTA and benzonitrile to the charging medium, as seen from Figs 8 and 9, respectively. Figure 8 gives the effect of 8.4 mM of BTA in 0.5 M H_2SO_4 on the fracture behaviour. Figure 8a shows a granular flat fracture region surrounded by a thick shear-lip. The granular

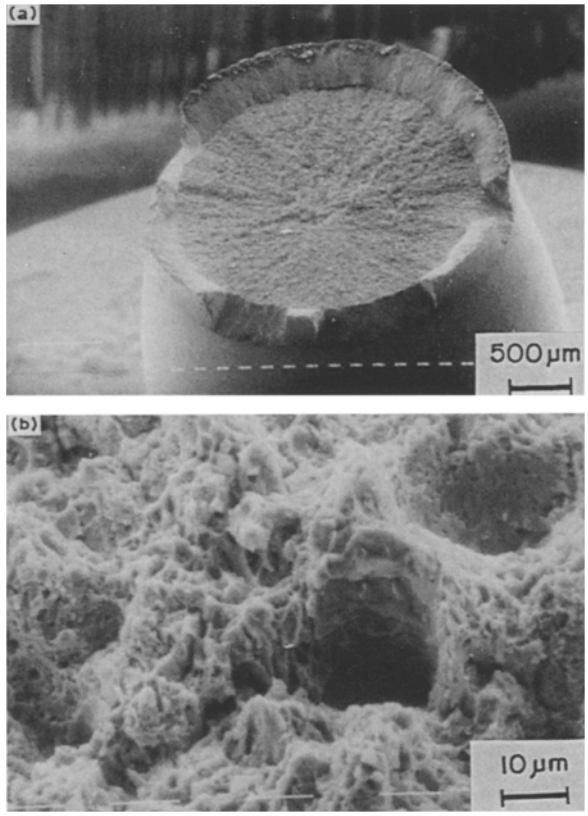

Fig. 6. Fracture surface of uncharged AISI 410 steel. Tensile tested at 5 × 10^{-5} s^{-1}.

region gave a rough fracture surface containing many deep holes. At high magnifications (Fig. 8b), flat facets indicative of quasi-cleavage are seen along with fine microvoids. These features support the relatively larger ductility exhibited by the steel hydrogen charged from BTA inhibited acid (Table 4).

Figure 9 gives the fractographic features observed on a specimen hydrogen charged from H_2SO_4 contain-

Table 4. Mechanical properties of air-hardened AISI 410 steel, cathodically hydrogen charged for 4 h from 0.5 M H_2SO_4 with various concentrations of inhibitor; c.d. = 10 mA cm^{-2}

S. No.	Medium of charging inhibitor concentration /mM	UTS(σ_F) /MPa	El. /%	RA /%	Loss in ductility /%		Embrittlement efficiency /%	
					El.	RA	El.	RA
1.	Air hardened (uncharged)	1440	17.0	46.0	–	–	–	–
2.	H-charged from 0.5 M H_2SO_4	1342	2.0	1.0	88.24	97.83	–	–
3.	0.5 M H_2SO_4 + Benzotriazole							
	0.17	1410	2.0	2.0	88.24	95.65	0.00	2.22
	0.84	1378	2.2	2.0	87.06	95.65	1.33	2.22
	4.20	1310	5.0	10.0	70.59	78.26	20.00	20.00
	8.40	1410	5.5	20.0	67.65	56.52	23.33	42.22
4.	0.5 M H_2SO_4 + Benzonitrile							
	0.390	1430	2.5	2.0	85.29	95.65	3.33	2.22
	0.974	1398	4.0	4.5	76.47	90.22	13.33	7.77
	4.870	1390	7.0	9.0	58.82	80.43	33.33	17.78
	9.740	1240	7.5	15.0	55.88	67.39	36.67	31.11

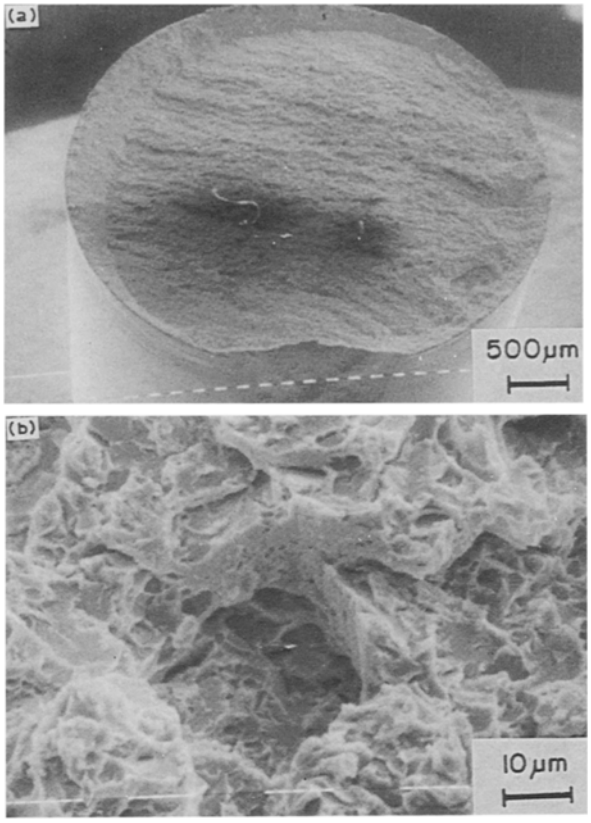

Fig. 7. Fracture surface of AISI 410 steel cathodically hydrogen charged from 0.5 M H_2SO_4 for 4 h, tensile tested at $5 \times 10^{-5} s^{-1}$.

ing benzonitrile. Here again the fracture appears to be highly brittle. Figure 9a shows that there is some reduction in area of the specimen at the fracture region and a peripheral shearlip is clearly visible in this

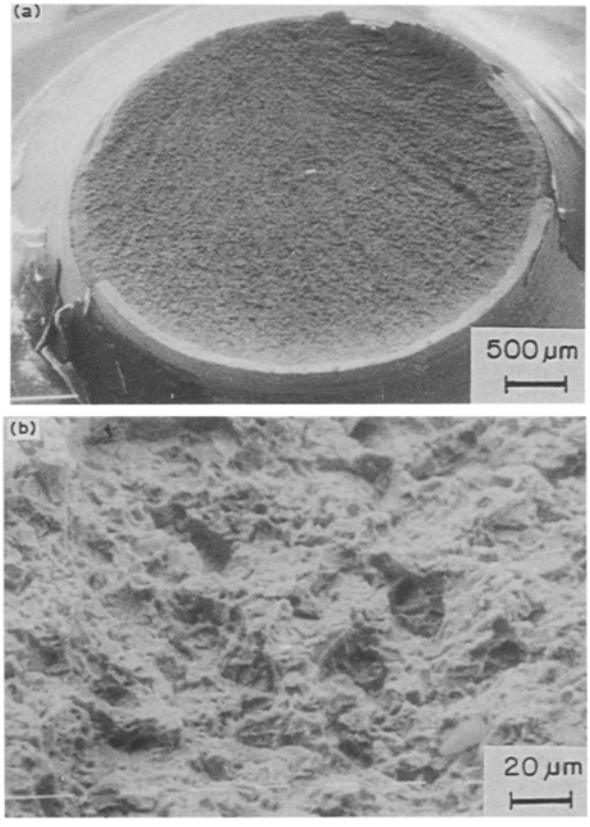

Fig. 8. Fracture surface of AISI 410 steel hydrogen charged from 0.5 M H_2SO_4 + 8.4 mM benzotriazole for 4 h, tensile tested at $5 \times 10^{-5} s^{-1}$.

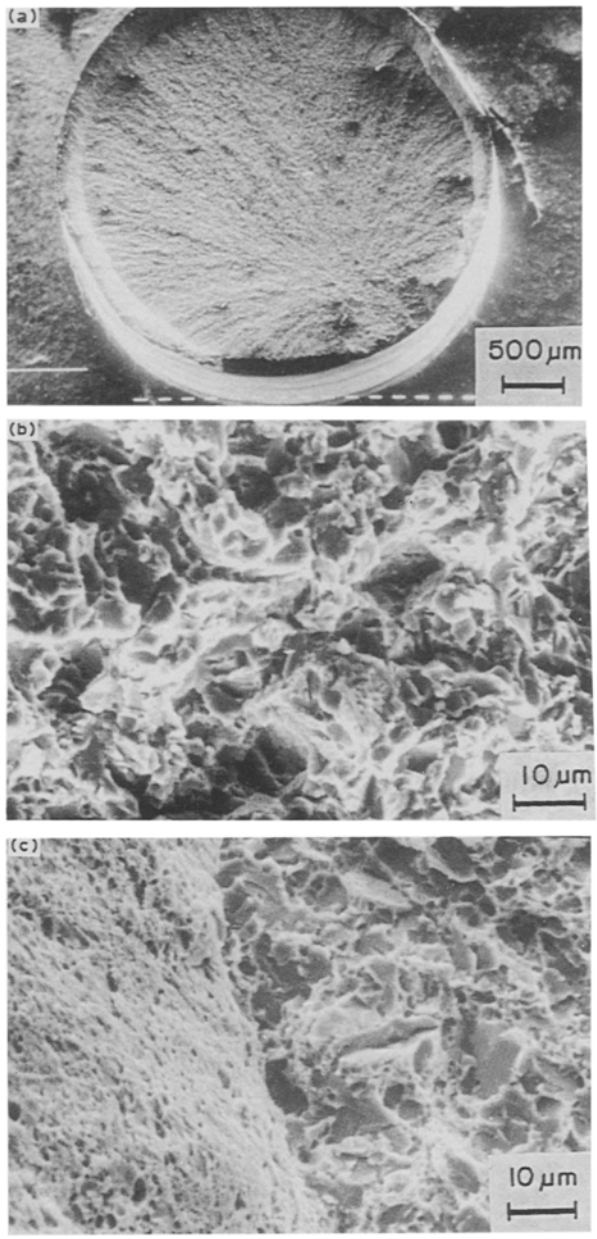

Fig. 9. Fracture surface of AISI 410 steel hydrogen charged in 0.5 M H_2SO_4 + 9.74 mM benzonitrile for 4 h, tensile tested at $5 \times 10^{-5} s^{-1}$.

picture. This indicates that the presence of benzonitrile has imparted some ductility to the material which is also evident from the increase in ductility seen in Table 4. The flat fracture region showed brittle quasi-cleavage fracture mode as seen from Fig. 9b. Figure 9c shows that some local plasticity exists even in the flat fracture region. Small microvoids are seen distributed among the quasi-cleavage facets.

4. Discussion

Inhibition of the corrosion of steel by organic molecules is possible by adsorption [32]. Adsorption of organic molecules on a metal surface depends upon the chemical nature of the inhibitor molecule, the environment, the nature of the metal surface and the electrochemical potential of the metal. Chemisorption of organic molecules takes place by the formation of a bond between the metal and adsorbed molecules

which depends on the nature of the metal and molecular structure of the inhibitor. Inhibitor molecules with double and triple bonds interact with the metal by π bond orbitals.

The adsorption characteristics of benzotriazole and benzonitrile was evaluated from the inhibition efficiency data given in Tables 2 and 3. It was found that both these compounds adsorb on the 410 steel surface according to the Temkin adsorption isotherm [33].

Corrosion inhibition of the steel by nitrile compounds in H_2SO_4 is well known [34]. As the electron density on the functional group increases, it is adsorbed strongly on the metal surface. From their molecular structures, it may be deduced [33] that the nitrogen atom of benzonitrile has a higher electron density due to delocalization of electrons than that of benzotriazole. This helps benzonitrile to adsorb more efficiently on the steel surface than benzotriazole and gives better inhibition efficiency than the latter (see Tables 2 and 3).

Hydrogen evolution is slowed down by the addition of these inhibitors but the mechanism of hydrogen evolution remains unchanged as they show the same cathodic slope.

Saito and Nobe [35] have shown that benzotriazole decreases the rate of hydrogen penetration into iron from 0.5 M H_2SO_4 remarkably and its effect decreases at applied current below 4 mA cm^{-2}. Measurements of the diffusion coefficient of hydrogen in iron in the presence of BTA indicated a simple adsorption of this organic compound. This implies that the rate of hydrogen penetration decreases because the surface area accessible for hydrogen ion discharge is reduced as a result of blockage by adsorbed species. Similiarly Bockris *et al.* [36] have shown that valeronitrile, benzonitrile and naphthonitrile decrease the rate of hydrogen permeation in steel exposed to acid solutions because of the vertical adsorption of these compounds on the surface of the metal which hinders the discharge of hydrogen ions. These compounds form strong $M-H_{ads}$ bonds which lower the permeation rate of hydrogen. It was observed that both these compounds reduce the hydrogen uptake by 410 steel when charged from 0.5 M H_2SO_4 solution [33] in conformity with the above findings. Thus it may be inferred that benzotrizole and benzonitrile reduce the amount of hydrogen absorbed by the 410 steel, thereby reducing its hydrogen embrittlement.

5. Conclusion

The following conclusions may be drawn from the present investigation:

1. Benzotriazole and benzonitrile decreased the hydrogen evolution current at cathodic potentials and inhibited corrosion of hardened 410 stainless steel in 0.5 M H_2SO_4. Benzonitrile was found to be a better corrosion inhibitor than BTA.

2. Benzotriazole and benzonitrile inhibited the hydrogen embrittlement susceptibility of the steel to some extent. The tensile ductilities of the charged steel were increased 2 to 3 times. The inhibition efficiencies increased with increasing concentration.

Acknowledgements

One of the authors (RA) thanks the Council of Scientific and Industrial Research, India, for financial assistance.

References

[1] R. S. Treseder and T. M. Swanson, Corrosion, **24** (1968) 31.
[2] A. J. Sedricks, 'Corrosion of stainless steels', John Wiley & Sons, New York (1979).
[3] F. Mancia, *Corros. Sci.* **27** (1987) 1225.
[4] A. K. Agrawal, W. N. Stiegelmeyer and J. H. Payer, *Met. Perf.* **26** (1987) 24.
[5] A. Cigada, T. Pastore, P. Pedeferri and B. Vicentini, *Corros. Sci.* **27** (1987) 1213.
[6] F. Mancia, CSM Internal Report No. 5243R (1985).
[7] R. D. Kane, M. Watkins and J. B. Greer, *Corrosion* **33** (1977) 231.
[8] H. H. Uhlig, *Met. Progress* **57** (1950) 486.
[9] P. Lillys and A. E. Nehrenberg, *Trans ASM* **48** (1956) 327.
[10] J. P. Bressanelli, *ibid.* **58** (1965) 3.
[11] J. Oredsson and S. Bernhardsson, Mat. Perf. **22** (1983) 35.
[12] B. Bazzoni, A. Cigada, L. Lazzari and P. Pedeferri, *Werkst. Korros.* **36** (1985) 151.
[13] H. A. El-Sayed, V. K. Gouda, *Corros. Prev. Control* **33** (1986) 142.
[14] A. Ikeda, M. Ueada and S. Mukai, Proceedings of the International Corrosion Forum, Corrosion/83, Anaheim, Paper No. 45 (1983).
[15] A. K. Dunlop, H. L. Hassell and P. R. Rhodes, Proceedings of the International Corrosion Forum, Corrosion/83, Anaheim, Paper No. 46 (1983).
[16] T. Yamada, M. Tustui, *Nagoya-Shikogyo, Kenkyuso Kenkyu Hokoku* (Res. Rep. Nugoya Munic, Int. Res. Inst.) **70** (1985) 9.
[17] J. P. Fraser and R. S. Treseder, *Corrosion* **8** (1952) 342.
[18] N. S. Rawt, G. Udayabhanu and R. K. Arora, *Trans. SAEST* **20** (1985) 63.
[19] I. Singh, A. K. Lahiri and V. A. Altekar, *Trans. IIM* **27** (1974) 125.
[20] G. Schmitt and B. Olbertz, *Werkst. Korros.* **29** (1978) 451.
[21] V. A. Marichev, *Prot. Met.* **21** (1985) 575.
[22] R. Agrawal and T. K. G. Namboodhiri, *Corros. Sci.* **30** (1990) 37.
[23] I. L. Rozenfeld, 'Corrosion Inhibitors', McGraw-Hill, New York (1981).
[24] L. G. Kors, S. M. Beloglazov, M. V. Ostrovskaya and G. F. Bebikh, *Korroz. Zashch Met.*, Kaliningrad **6** (1983) 54.
[25] S. H. Sanad, *Surf. Technol.* **22** (1984) 20.
[26] V. F. Volosoin, O. P. Golosova and L. A. Mazalevskaya, *Zashch Met.* **22** (1986) 472.
[27] B. S. Chaudhari and T. P. Radhakrishnan, 10th International Congress on Metallic Corrosion, India, **3** (1987) 2327.
[28] H. H. Uhlig, Corrosion and Corrosion Control, John Wiley & Sons, New York (1964).
[29] A. Kozlowska, H. Kryszezynska, E. Radomska, B. Szeptycka and S. Wlodarczyk, Powloki Ochr **14** (1986) 8.
[30] R. J. Chin and Ken Nobe, *J. Electrochem. Soc.* **118** (1971) 545.
[31] T. K. G. Namboodhiri *Trans. IIM* **37** (1984) 764.
[32] H. Fischer, Proceedings of the European Symposium on Corrosion Inhibitors, Ferrara, Italy (1960) 1.
[33] Reeta Agrawal, Ph.D. Thesis, Banaras Hindu University (1990).
[34] J. Vosta, G. Trabanelli, J. Pelikan, F. Zucchi and V. Hluchan, Proceedings of the 9th International Congress on Metallic Corrosion, Canada (1984) 378.
[35] Y. Saito and K. Nobe, *Corrosion* **36** (1980) 178.
[36] J. O'M. Bockris, J. McBreen and L. Nanis, *J. Electrochem. Soc.* **112** (1965) 1025.